DECLARATION

This work is original and has not been previously submitted in support of a Degree qualification or other course.

Signed ……Brecken Elizabeth Calhoon…….

Date…02/10/2019…..

Word count: 4188

Research Article

AKR1C3 inhibition by curcumin, demethoxycurcumin, and bisdemethoxycurcumin: an investigation

Brecken Calhoon

Abstract

Background: Aldo-keto reductase 1C3 (AKR1C3) has been shown to be overexpressed in cancers due to its regulatory roles in cell proliferation and differentiation. Curcumin, known to have anti-tumour properties, and its analogues demethoxycurcumin (DMC) and bisdemethoxycurcumin (BDMC) were studied to determine their inhibitory effects on the AKR1C3 enzyme.

Methods: AKR1C3 was purified and analysed to determine its protein concentration in transformed *Escherichia coli (E. coli)* cells. Enzyme assays equaling 1 mL contained 2.82 mg/mL AKR1C3, 50 µM of 3 mM NADPH, and varying volumes of potassium phosphate (50 mM, pH 6.5), 9,10-phenanthrenequinone (PQ), and inhibitors were measured at 340 nm. The V_{max}, K_m, K_I, and σ^2 of AKR1C3 in the presence and absence of inhibitors were determined using a non-linear regression analysis on Fig.P Software.

Results: PQ alone found V_{max} = 0.47 IU/mg, K_m = .435 µM, K_i = 6.29 µM, and σ^2 = 0.946. Inhibitor potency was BDMC > DMC > curcumin in the presence of 1 µM PQ. Further analysis of BDMC indicated mixed inhibition (V_{max} = 0.46 IU/mg, K_m = .406 µM, K_i = 1.59 µM, and σ^2 = 0.970). Further analysis of PQ at higher concentrations found a divergence from Michaelis-Menten kinetics, with a decrease in AKR1C3 activity after V_{max} was reached.

Conclusions: BDMC was the more potent inhibitor of AKR1C3 in transformed *E. coli* compared to DMC and curcumin. The results suggest mixed inhibition of AKR1C3 in the presence of BDMC. Additional analysis of PQ at higher concentrations saw a loss of Michaelis-Menten kinetics as the activity of AKR1C3 decreased after reaching V_{max}. This requires further examination.

Keywords: Aldo-keto reductase 1C3 (AKRIC3); curcumin; demethoxycurcumin (DMC); bisdemethoxycurcumin (BDMC)

Introduction

Aldo-keto reductase 1C3 (AKR1C3) is a 36.8 kD member of the aldo/keto reductase superfamily AKR1C that catalyses alcohols from aldehydes and ketones in the presence of NAD(P)H [1]. AKR1C3 has an influential role in several cell signalling pathways that can influence cell proliferation and differentiation. Prostaglandins (PG) PGH_2 and PGD_2 are converted to $PGF_{2\alpha}$ and 9α,11β-$PGF_{2\alpha}$, respectively, in the presence of AKR1C3 (Fig. 1a) [2, 3], while weak androgens and oestrogens (4-androstone-3,17-dione and oestrone) are converted into potent ones

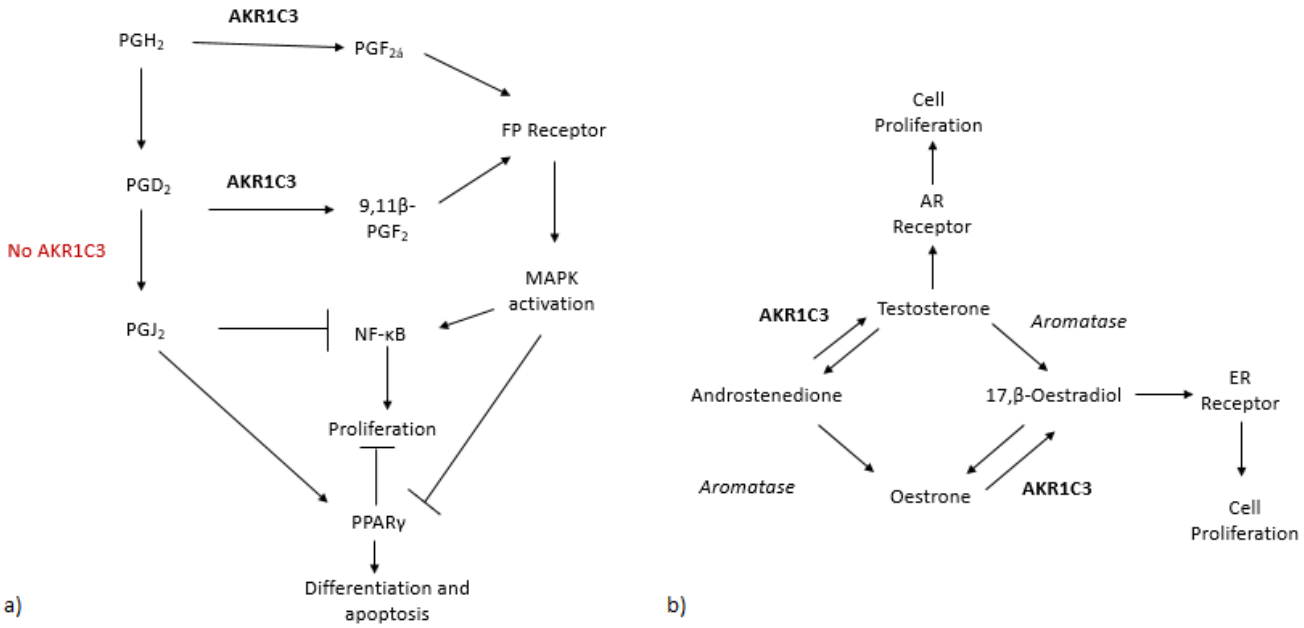

Figure 1. AKR1C3 influence over cellular pathways. **(a)** Prostaglandin synthesis in the presence and absence of AKR1C3. **(b)** Androgen synthesis in the presence of AKR1C3. Abbreviations: Aldo-keto reductase 1C3 (AKR1C3; Androgen receptor (AR); Oestrogen receptor (ER); Mitogen-activated protein kinase (MAPK); Nuclear factor κB (NF-κB); Peroxisome proliferator-activated γ receptor (PPARγ).

(testosterone and 17β-oestradiol) due to the co-activation of the androgen receptor (AR) and oestrogen receptor (ER) (Fig. 1b) [4, 5].

These conversions can be problematic in tumorous cells, as the resulting products can influence the rate of gene transcription [6]. Overactivation of gene transcription due to AKR1C3 overexpression has been found in a myriad of cancers including breast, colon, colorectal, endometrial, prostate, and acute myeloid luekeaima [7, 8]. In the absence of AKR1C3 PGD_2 can be converted to 15-deoxy-$\Delta 1^{2,14}$-PGJ_2 (PGJ_2), which can bind to the peroxisome proliferator-activated receptor (PPAR) γ [9, 10]. PPARγ is then able to promote cellular differentiation and apoptosis [9]. This relationship between AKR1C3 and cell signalling pathways suggests overexpression of tumorous cells could be impeded with the inhibition of AKR1C3.

Curcumin(Fig. 2a), a polyphenol from the rhizome of the turmeric plant, has been shown to contain anti-inflammatory, antioxidant, and anti-tumorous activities [11]. Several *in vitro* and *in vivo* studies have been performed to determine curcumin's efficacy as a therapeutic option for cancer [12-14]. However, due to its poor bioavailability and stability *in vivo* [12, 15-16], it has not seen much success in clinical trials. As such, curcumin analogues have been used to greater effect.

The naturally occurring curcumin analogues demethoxycurcumin (DMC) (Fig. 2b) and bisdemethoxycurcumin (BDMC) (Fig. 2c), have not been examined in the AKR1C superfamily, but have tested on cancer cells to a positive effect [17]. BDMC has also shown to be more stable in rat livers than curcumin and DMC [15]. This suggests BDMC may have a greater bioavailability as well. While curcumin has been studied in prostate cells on AKR1C2 activity [18], neither curcumin, DMC, nor BDMC has been utilised to inhibit AKR1C3 activities, despite AKR1C3 overexpression in a variety of cancers.

This study aimed to examine the inhibitory effects of curcumin, DMC, and BDMC on AKR1C3 expression in transformed *Escherichia coli* (*E. coli*) cells and determine the type of inhibition that occurred. Such evidence could provide future studies with valuable information for the development

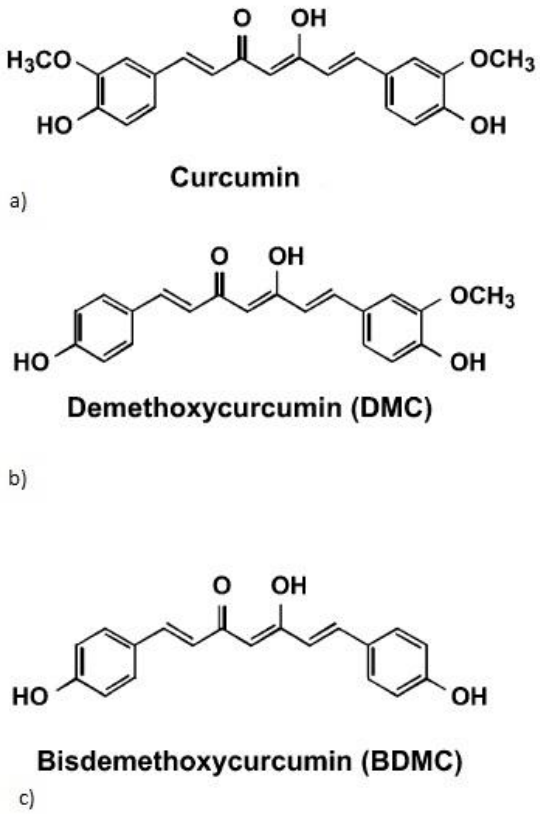

Figure 2. Chemical structure of curcumin **(a)**, demethoxycurcumin **(b)**, and bisdemethoxycurcumin **(c)** [13].

and optimisation of curcumin-based therapeutics in cancer patients.

Methods

Cell Culture and Purification

E. coli cells BL21(DE3) (New England Biolabs UK) containing the human AKR1C3 enzyme (pET21b-AKR1C3) with a His-tag were grown overnight in an orbital shaker at 300 RPM and 37°C and transferred into three 6 mL bottles of L-broth and ampicillin $(Amp)^R$ (100 µg/mL). Cells were shaken and grown overnight at 37°C before transferring into 400 mL L-broth+Amp and centrifuged for 45 minutes at 4500 RPM. The resulting pellet was stored at -80°C.

The pellet was resuspended in accordance with the manufacturer's instructions upon addition of 8 mL of BugBuster, a protease inhibitor cocktail tablet, supplied by Sigma-Aldrich (Darmstadt, Germany). Upon removal from the room temperature water bath, the suspension was extracted and set aside as Solubilised Bacteria (SB). The remaining sample was split into two eppendorf tubes and spun at 30,000 g for 25 minutes at 10°C. The resulting supernatant was removed and set aside as Supernatant (Sup). Both the Sup and SB were frozen. The homogenate was further purified using a His-select Ni^{2+} resin column (Sigma-Aldrich, Darmstadt, Germany) per the manufacturer's instructions. The wash buffer comprised of 50 mM sodium phosphate monobasic monohydrate at 300 mM NaCl, pH 8.0, while the elution buffer additionally contained 100 mM of Imidazole, pH 8.0. Eight elutions of 1 mL were collected and analysed for protein (P) concentration.

Protein Estimation

A standard curve was created using a Bradford Assay and bovine serum albumin (BSA) from Bio-Rad Laboratories, as seen in the supplementary material (Fig. 1). SB, Sup, and P samples were additionally analysed (10 µL of sample, 40 µl distilled water, and 950 µL of Bradford Reagent). All measurements were taken at 595 nm on a Jenway 7200 visible spectrophotometer (Stone, Staffordshire, UK) and performed in triplicate.

To determine the protein concentrations of AKR1C3 in SB, Sup, and P, each sample was diluted to 1 mg/ml with distilled water. The samples were further diluted to 0.5 mg/mL [100 µL sample, 100 µL sample buffer (Sigma S3401, Sigma-Aldrich, Darmstadt, Germany), and 100 µL Laemmli Blue]. They were then heated at 90°C for approximately 7 minutes and placed on ice before electrophoresis was performed.

Gel Electrophoresis

The Bio-Rad Laboratories gel electrophoresis tank was assembled and loaded according to the manufacturer's instructions. SB, Sup, and P samples were loaded at 10 µg per lane. The gel was run at 150 V for 45 minutes before being left overnight in 30 mL of EZ blue staining reagent (Sigma-Aldrich, Darmstadt, Germany).

Activity of AKR1C3

Protein activities of AKR1C3 were determined by measuring the oxidation of NADPH (ε = 6220 M^{-1} cm^{-1}) at 340 nm on a Jenway 7315 spectrophotometer (Stone, Staffordshire, UK) at room temperature. The NADPH solution had been made in distilled water from a 1M NADPH stock to achieve a final concentration of 3 mM. The resulting solution was made slightly alkaline with the addition of NaOH (4 µL) to stabilise said solution. The assay buffer was potassium phosphate (50 mM, pH 6.5). The binding substrate was 1 mM stock of 9,10-phenanthrenequinone (PQ) in dimethyl sulfoxide (DMSO). 50 µL of 3 mM NADPH was used for every assay, while 20 µL of 2.82 mg/mL AKR1C3 was also used. Volumes of potassium phosphate, PQ, and inhibitors varied to ensure the total volume of the enzyme reaction was equal to 1 mL.

AKR1C3 Inhibitors

The inhibitors curcumin, DMC, and BDMC were added once a Michaelis-Menten curve was established for AKR1C3 activity with PQ as its substrate. A 10 mM solution of curcumin was made in 5 mL DMSO . 10 mM solutions of DMC and BDMC were both products of Sigma-Aldrich (Darmstadt, Germany). All three inhibitors were kept out of the light and stored in 4°C. The total volume of buffers, substrates, AKR1C3, and inhibitors always was equal to 1 mL.

Statistical Analysis and Imaging

A non-linear regression analysis was performed to determine the V_{max}, K_m, K_I, and σ^2 of AKR1C3 activities using Fig.P Software (Hamilton, Ontario, Canada). These constants were found with PQ concentrations up to 25 µM and BDMC up to 50 µM.

Protein purification intensity was analysed using Image Processing and Analysis in Java (Image J) (National Institute of Health, Maryland, USA). AKR1C3 structure was rendered using Visual Mode Dynamics Imaging Software (University of Illinois, Urbana-Champaign, USA). The code was obtained from the Protein Data Bank, file number 1RY0.

Results

Protein Purification

The AKR1C3 enzyme was purified and eluted into eight different eppendorf tubes. The elution profile (Fig. 2 supplementary material) shows the highest protein concentration of AKR1C3 was collected during the second and third elutions, which were pooled together. The resulting gel (Fig. 3) showed the purified AKR1C3 to be roughly 35.5 kD, which is near the approximate molecular mass of 37 kD for AKR1C3, indicating the protein has been successfully purified. The Sup and SB also had bands around 35.5 kD, in addition to bands with greater and less molecular weight.

Determination of Unknown Samples

The protein concentrations of SB, Sup, and P (Table 1) were calculated based upon the BSA standard curve found in Figure 1 of the supplementary material. These concentrations were then used to calculate the amount of protein per volume in the subsequent enzyme assays.

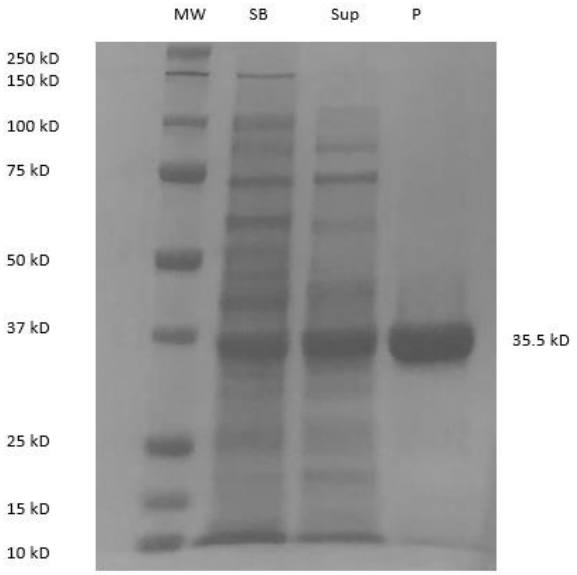

Figure 3. Electrophoresis of unknown samples. Thick bands around 37 kD indicate the presence of AKR1C3. Abbreviations: Molecular Weight (MW), Solubilised Bacteria (SB), Supernatant (Sup), and Purified Protein (P).

Table 1. Unknown protein sample concentrations. Concentrations of unknown protein within the purified protein, solubilised bacteria, and supernatant. Concentrations determined from the BSA standard curve.

unknowns (10 µL sample + 40 µL water)	Mean Absorbance (595 nm)	SD	CV	Concentration (mg/mL)
Purified Protein	0.721	0.01914	0.026534	2.82
Solubilised Bacteria	0.746	0.01159	0.01553	2.92
Supernatant	0.504	0.01097	0.02178	1.94

Enzyme Assays

The activity of AKR1C3 was determined by measuring the absorbance of the oxidation reaction of NADPH at 340 nm. The mean absorbance was used to calculate the activity via the equation:

$$\text{Activity (IU/mg)} = \frac{(\text{Absorbance/min})(1000)}{(6220\ M^{-1}\ cm^{-1})(\text{mg of protein})}$$

The rates of activity were then graphed to determine the V_0, V_{max}, K_m, and K_I from the resulting Michaelis-Menten curve and Lineweaver-Burk plots. On the Michaelis-Menten curve, V_{max} is the maximum velocity the enzyme reached, while the K_m is one half of V_{max}. These could then be used to determine V_0 from the equation:

$$V_0 = V_{max}\left\langle \frac{[\text{Substrate}]}{[\text{Substrate}] + K_m} \right\rangle$$

The type of inhibition was confirmed by Lineweaver-Burk plot equation:

$$\frac{1}{V_o} = \frac{K_m}{V_{max}} \cdot \frac{1}{[S]} + \frac{1}{V_{max}}$$

which was able to show if V_{max} or K_m was altered in reactions performed in the presence of an inhibitor. K_I could also be calculated by the equation:

$$V_0 = \frac{V_{max}}{\left(1 + \frac{[I]}{K_I}\right)}$$

whereby [I] was the concentration of the inhibitor.

AKR1C3 with Substrate PQ

Reactions with AKR1C3, NADPH, and PQ were measured using 20 µL of AKR1C3 (2.82 mg/mL) and PQ concentrations ranging from 0.25 µM to 10 µM. The resulting mean activities of AKR1C3 formed a Michaelis-Menten curve (Fig. 4a), where K_m = 1.84 (µM) and V_{max} = 0.561 (IU/mg). This was calculated from the equation

$$y = 3.273x + 1.7819$$

(R^2 = 0.9776) as found from the Lineweaver-Burk plot (Fig. 4b). The Lineweaver-Burk plot was also established as the baseline activity of AKR1C3 with PQ to compare it with further reactions involving inhibitors.

AKR1C3 and Inhibitors

Using the value of the Michaelis-Menten constant, K_m, for PQ, the activity of AKR1C3 was tested in the presence of 1 µM PQ and varying concentrations of curcumin, DMC, and BDMC ranging from 0.25 µM to 80 µM. Raw data can be found in the supplementary information. Figure 5 shows the activity percentage of curcumin, DMC, and BDMC, as the daily AKRC13 and PQ only standard would vary based on the room temperature.

The data suggested BDMC was the most effective inhibitor, with almost complete inhibition of AKR1C3 activity at 30 µM (Fig. 5c), followed by DMC with no AKR1C3 activity at 80 µM (Fig. 5b). Curcumin is the least effective, with some AKR1C3 activity still occurring at 75 µM (Fig. 5a). BDMC and

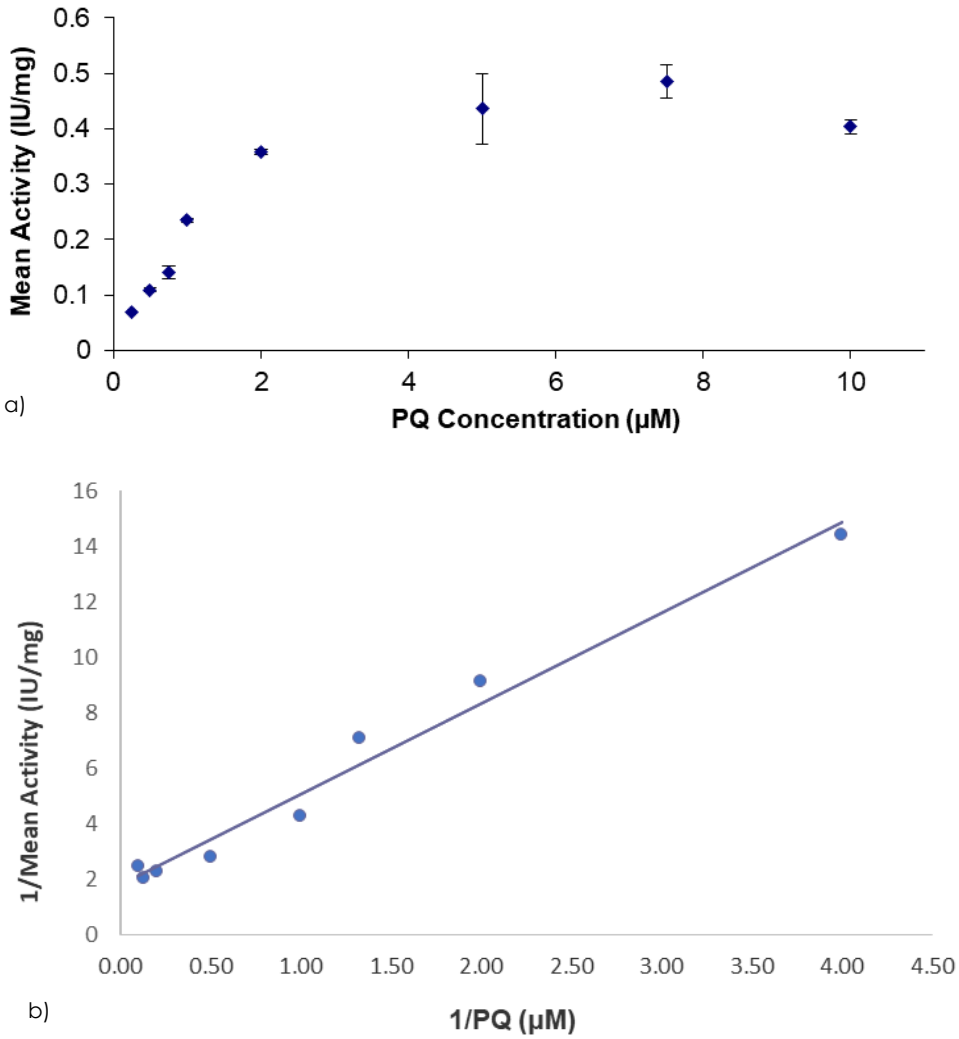

Figure 4. Mean Activity of PQ up to 10μM. Calculations based upon 20μL of purified AKR1C3 (n = 3 – 5). Error bars indicate standard deviation. **(a)** Michaelis-Menten curve where K_m = 1.84 μM and V_{max} = 0.561 (IU/mg) **(b)** Lineweaver-Burk plot where the equation y = 3.273x + 1.7819 (R^2 = 0.9776).

DMC also appeared to have a steeper gradient, suggesting a higher V_0 (Fig. 5d). As BDMC was the more potent inhibitor, it was used for further experimentation.

AKR1C3, PQ, and BDMC

Having established that BDMC was our most potent inhibitor, the activities of AKR1C3 with a varying substrate concentration and constant inhibitor concentration were measured. 10 μM of BDMC was used, as it was approximately halfway between complete and no inhibition of AKR1C3. PQ concentrations ranged from 0.5 μM to 5 μM.

Interestingly, there was a peak of activity around 1 μM PQ, and then decreasing rates of activity until it was almost non-existent (Fig. 6a). This result, combined with a data-point at 10 μM for PQ alone (Fig. 4a), led us to extend the analysis of PQ alone with AKR1C3.

AKR1C3 and PQ up to 25 μM

A final measurement of 25 μM PQ with no inhibitors found the activity of AKR1C3 had decreased, in divergence with Michaelis-Menten kinetics (Fig. 6b). Using the equation

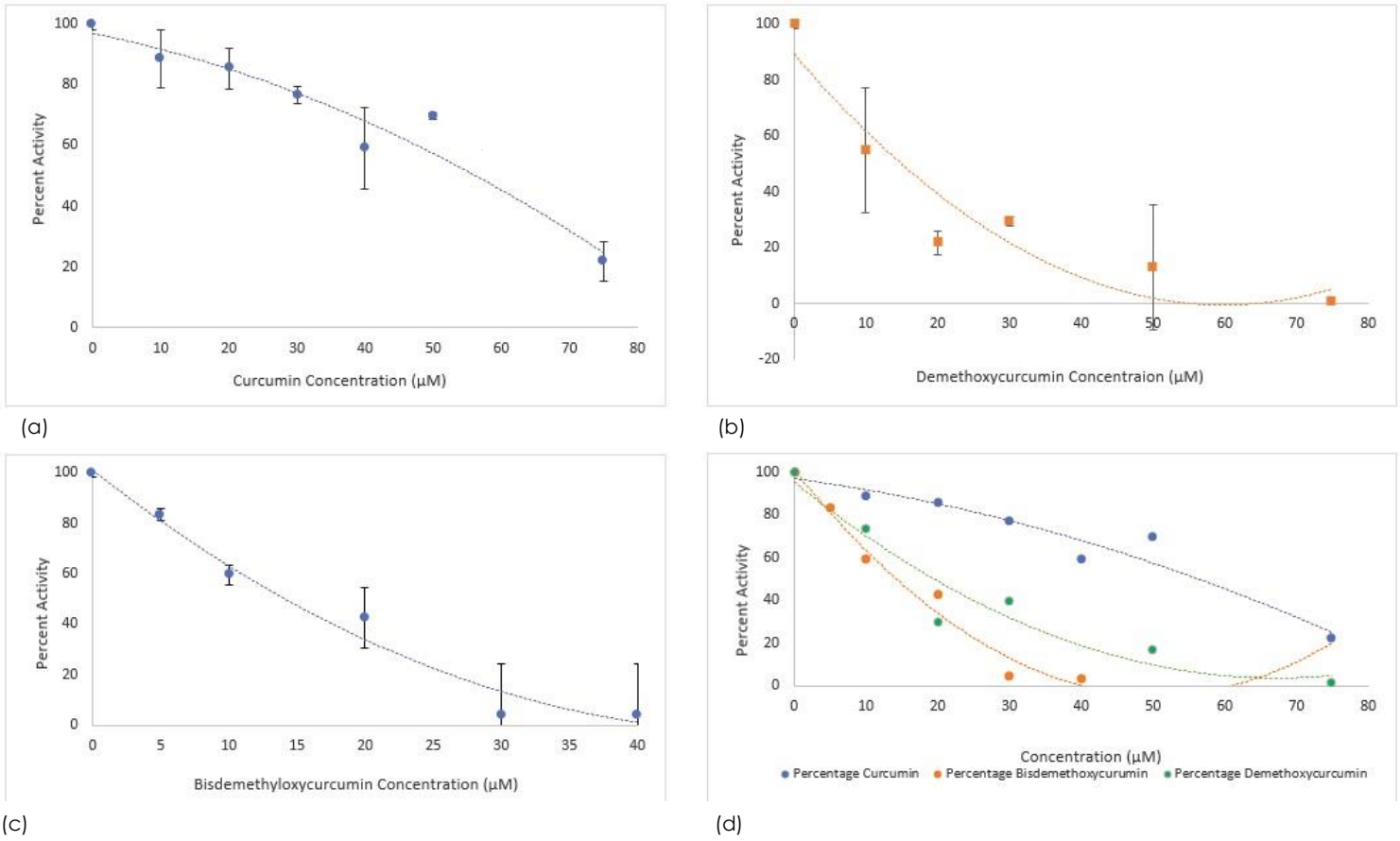

Figure 5. Activity (IU/mg) percentages of (a) Curcumin (R^2 = 0.9346), **(b) Bisdemethoxycurcumin** (R^2 = 0.9768), **(c) Demethoxycurcumin** (R^2 = 0.8964) **and (d) Combined when administered in conjunction with 1μM PQ.** Activity of AKR1C3 decreases with increasing concentrations of the inhibitors (n = 2 – 5). Error bars indicate the coefficient of variation.

$$V_0 = V_{max}\left\langle \frac{[Substrate]}{[Substrate] + K_m} \right\rangle + \left(\frac{V_{max}}{1 + \frac{[I]}{K_i}} \right)$$

analysis of AKR1C3 and PQ alone found V_{max} = 0.47 IU/mg, K_m = .435 μM, K_i = 6.29 μM, V_0 = 0.09 IU/mg and σ^2 = 0.946 (Fig. 7a), while AKR1C3, 1 μM PQ, and up to 50 μM BDMC resulted in V_{max} = 0.46 IU/mg, K_m = .406 μM, K_i = 1.59 μM, V_0 = 0.33 IU/mg and σ^2 = 0.970 (Fig. 7b). This indicated mixed inhibition of AKR1C3 by BDMC.

Discussion

The enzyme AKR1C3 has been found to be overexpressed in a variety of cancers and diseases [7, 8], indicating that it has a regulatory role in cell proliferation and differentiation. Theoretically, the ability to inhibit AKR1C3 overexpression could prevent disease progression and possibly result in remission. Curcumin and its analogues have shown anti-tumour and anti-inflammation properties [11] but has not been specifically studied in the inhibition of AKR1C3. The relationship between the inhibitory agents curcumin, DMC, and BDMC AKR1C3 was thereby explored using PQ as a substrate and NADPH as a co-activator.

We observed inhibitory activity at concentrations as low as 10 μM when applied in conjunction with 1 μM PQ. Inhibitory potency indicated BDMC > DMC > curcumin, which has been shown in matrix metalloproteinases (MMPs) and urokinase plasminogen activator (uPA) [18] but is contradictive to potency results targeting tumour necrosis factor (TNF)-induced nuclear factor κB (NF-κB) [13]. This suggests the structure of the target molecule for curcumin, DMC, and BDMC is significant in determining the potency of the three curcuminoids.

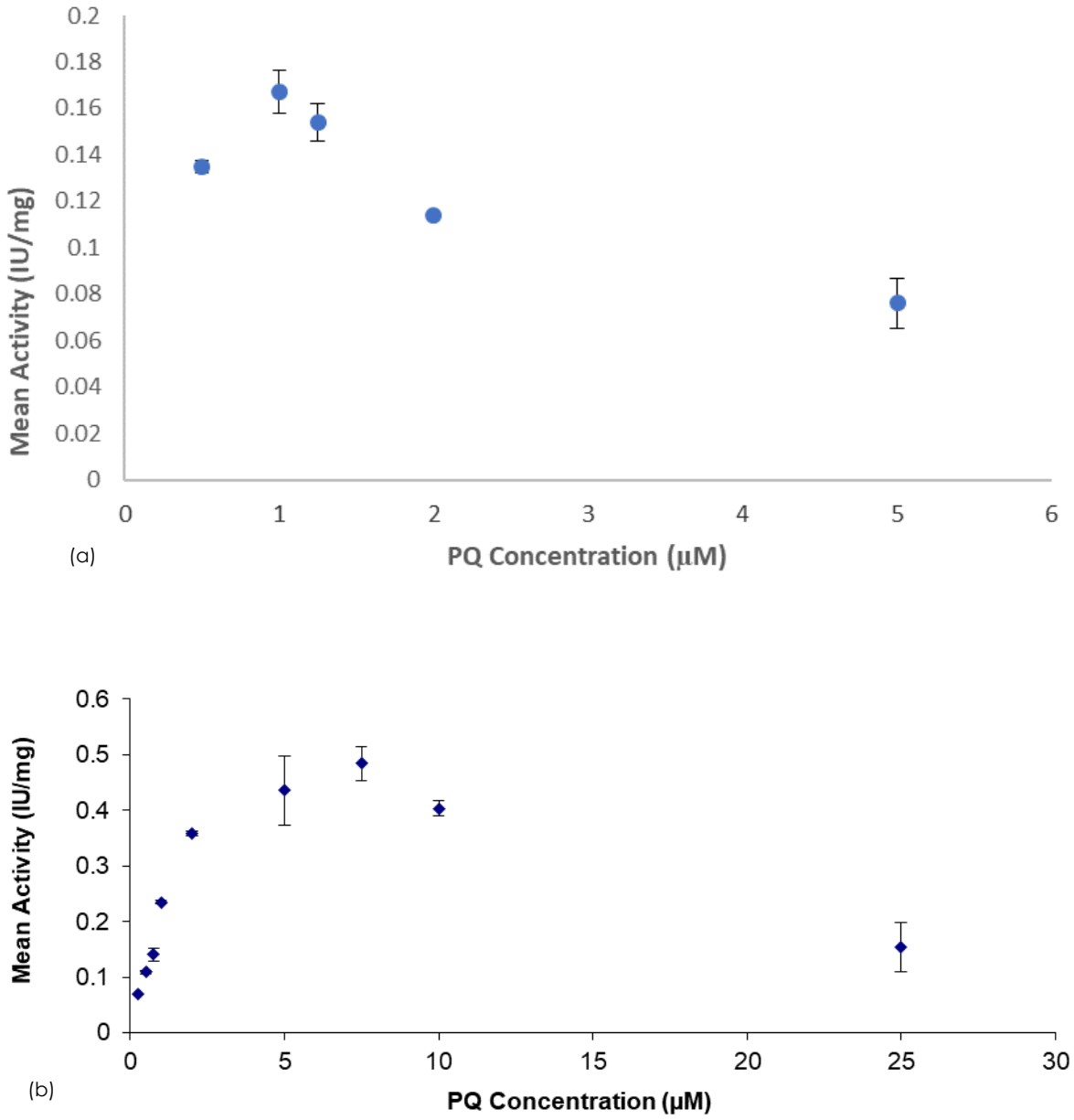

*F*igure 6. **PQ Activity (IU/mg) with and without BDMC. (a)** Activity of PQ + 10 µM Bisdemethoxycurcumin. PQ concentrations ranging from 0.5 µM to 5 µM. Error bars indicate standard deviation (n = 3 – 5) **(b)** PQ activity (IU/mg) up to 25 µM. Calculations based upon 20µL of purified AKR1C3. The decrease in activity suggests self-inhibition at greater concentrations. Error bars indicate standard deviation (n = 2 – 5).

Three amino acid loops near the active site of AKR1C3 allow for a flexibility in binding ligands, as does the existence of three sub-pockets within the active site (Fig. 8) [19, 20]. These subpockets vary in size and amino acid residues which provides multiple binding sites for ligands of different structures [20]. As curcumin, DMC, and BDMC only differ in the electron donating methoxy groups – curcumin has two in the ortho position, DMC has one, and BDMC contains none [13] – it would be expected that these methoxy groups affect the binding capabilities and potencies when applied to AKR1C3. The lack of one methoxy group in DMC and two in BDMC may increase the bioavailability, as seen in rat livers [15], due to the stability of the aryl rings on either side of the β-diketone moiety.

Historically, curcumin has been shown to display competitive and non-competitive inhibition within cells depending upon the target [21, 22]. Meanwhile, Lovering et al.

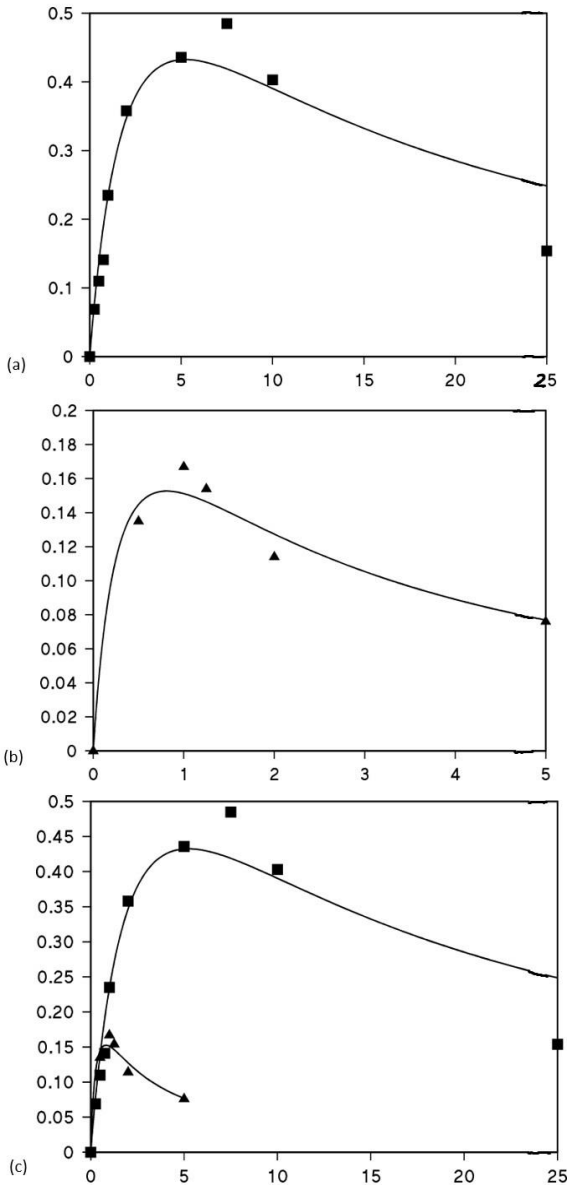

Figure 7. Activity (IU/mg) of AKR1C3. (a) AKR1C3 activity in the presences of PQ up to 25 µM. Vmax = 0.47 IU/mg, Km = .435 µM, and KI = 6.29 µM (σ^2 = 0.946) **(b)** Activity of AKR1C3 when 1 µM PQ is combined with Bisdemethoxycurcumin up to 50 µM. Vmax = 0.46 IU/mg, Km = 0.406 µM, and KI = 1.59 µM (σ^2 = 0.970) **(c)** Combined graphs of PQ and PQ + Bisdemethoxycurcumin (n = 2 – 5).

[19] has found mixed inhibition of the AKR1C3 enzyme using non-steroidal anti-inflammatory drugs (NSAIDs), which was suggestive of a second inhibitor-binding site on AKR1C3. These varying results imply AKR1C3 could be inhibited by curcumin in any manner. The current results indicated a type of mixed inhibition. Competitive inhibition was observed for the curcuminoids regarding AKR1C3, as there was essentially no change in the V_{max} for AKR1C3 in the presence of the inhibitor compared to without the inhibitor (V_{max} = 0.46 IU/mg and 0.47 IU/mg, respectively) while uncompetitive inhibition was observed in the decreased K_m value for the reaction with curcuminoids (K_m = .406 µM and .435 µM). Mixed inhibition of the curcuminoids when applied to AKR1C3 may be possible due to its elastic structure. This flexibility may also account for the unexpected activity we observed upon increasing the concentration of PQ and BDMC.

Results obtained when the concentration of BDMC remained constant at 10 µM and PQ concentrations ranged from 0.5 µM to 5 µM were surprising, as we predicted the activity of AKR1C3 to increase as we increased the concentration of PQ. However, our results showed peak activity of AKR1C3 occurred at 1 µM PQ, before a decrease in activity was observed at increasing concentrations, with almost no activity observed starting at 3 µM PQ. Subsequently, we increased the concentration of PQ in the absence of any inhibitor to observe the activity of AKR1C3 in the presence of higher substrate concentrations. This led to a discovery that our AKR1C3 enzyme did not follow Michaelis-Menten kinetics and began to decrease in activity upon reaching V_{max}.

This decrease in activity suggests AKR1C3 may be self-inhibiting once it has reached substrate saturation. This could be possible be due to a second inhibitor-binding site, as suggested by Lovering [19], which may be hidden until substrate saturation is achieved. Upon saturation, the malleable loops may reveal a self-inhibiting binding site that prevents AKR1C3 from overexpressing. This could also explain why there is AKR1C3 overexpression in some diseases and not others. Those with disease-causing AKR1C3 overexpression could have an inactive or inhibited potential concealed binding site that allows for self-inhibition of AKR1C3. Further analysis and data collection of AKR1C3 in combination with PQ and/or inhibitors must occur before serious conclusions can be

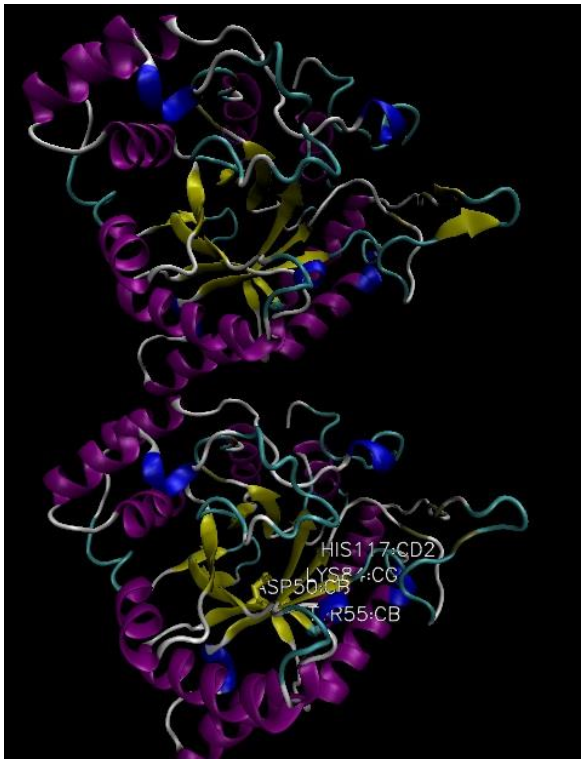

Figure 8. AKR1C3 structure. The catalytic tetrad within the active site is emphasized by Asp50, Tyr55, Lys84, and His117 residues. The loops around the active site and subpockets within allow for flexibility when binding ligands.

drawn, however. The crystal structure of AKR1C3 with PQ at saturated levels should also be studied before this theory can be substantiated.

Regardless of the mechanism of action for PQ and AKR1C3, we were able to observe the inhibitory effects of curcumin, DMC, and BDMC in concentrations ranging from 10-80 μM. This indicates these inhibiting curcuminoids could be tested on AKR1C3 tumour cells to determine their efficacy. Curcumin has already proven to elevate AKR1C2 expression in prostate cancer cells, leading to a decrease in tumour size [18]. This suggests curcumin and its analogues would be effective in binding to and inhibiting AKR1C3 activity in tumorous cells, as AKR1C2 and AKR1C3 share 84 percent similarity [1]. Curcumin and its analogues could theoretically bind to the active site of AKR1C3, as the carbonyl group in curcuminoids should form strong hydrogen bonds with the Tyr55 and His117 residues of AKR1C3. Tyr55 and His117 can act as an anchor in the active site for ligands that contain a carbonyl or carboxylate group, allowing for the reduction action to proceed [19, 23]. BDMC may also have increased stability due to the lack of methoxy groups on the aryl ring, as mentioned previously.

Inhibition of AKR1C3 by curcuminoids could potentially prevent excess cell proliferation by decreasing the amount of $PGF_{2\alpha}$ and 9α,11β-$PGF_{2\alpha}$ activating the prostaglandin F (FP) receptor via ligand binding to the receptor itself or binding to the Gq coupled FP receptor [24, 25]. This in turn would inhibit FP from activating, via downstream, cross-signalling events, receptor tyrosine kinases (RTKs), which lead to the activation of the mitogen-activated protein kinase (MAPK) and phosphatidylinositol 3-kinase (PI3K) pathways that target gene transcription [26]. Over-activation of the AR or ER by AKR1C3 can additionally cause gene overexpression due to its role as a DNA-binding transcription factor [27], suggesting inhibition would decrease the proliferation of androgen- and oestrogen-related diseases and cancers. Furthermore, inhibition of AKR1C3 has shown to increase PPARγ activity in cancerous cells, leading to increased cell differentiation and apoptosis [28-30]. This would imply that inhibition of AKR1C3 by curcuminoids would also increase PPARγ activity in tumour cells, leading to a reduction in tumour size.

Despite these encouraging results on the inhibitory activity of curcumin, DMC, and BDMC on AKR1C3, more data needs to be collected in a stable environment. As an enzyme, AKR1C3 is sensitive to temperature and pH. This was extremely evident in our experiments due to the inability to control the room temperature. Temperatures could range anywhere from 18°C to 26°C in our laboratory, which would affect the activity of AKR1C3. On warmer days the activity was typically higher than cooler days. However, we tried to mitigate this obstacle by measuring a daily standard of 1 μM PQ with no inhibitor and comparing the daily results to this standard. We would then calculate the daily activity compared

to our PQ standard curve (Fig. 4a), which was measured and calculated in one day.

Temperature, along with pH, has also shown to affect the whether the keto-enol tautomers of curcuminoids exist in their *trans* or *cis* form, thereby affecting their activity [31-33]. This again was observed in our results, as there was a change in inhibitor activity based upon the room temperature. We also noticed a difference in activity when a new potassium phosphate buffer was used, as the buffer was originally slightly more acidic (pH = 6.4) then the required pH for the buffer (pH = 6.5). This emphasised curcumin's sensitivity to pH, as it has shown to be more stable in acidic environments compared to neutral and basic [34], and less soluble in acidic and neutral environments compared to basic environments [35]. Such considerations must be contemplated when using curcumin or its derivatives as a therapeutic tool in humans, as there is a neutral-to-slightly basic physiological pH in blood and plasma.

Future experiments, in addition to being conducted in a stable environment, should collect more data points at different concentrations of PQ when applied in conjunction with a constant concentration of BDMC. As the more potent inhibitor in our experiment, BDMC can be used to establish if it is truly mixed inhibition occurring when applied to AKR1C3. Unfortunately, due to time and materials constraints, we were only able to collect five data points in duplicate for 1 µM PQ and varying BDMC concentrations. This was also true for 10 µM BDMC and varying PQ concentrations. It would also be beneficial to analyse the molecular components of the several-month old bottle of BDMC to see if any molecular degradation has occurred that could alter its activity. If so, this could be used as a model for a future curcumin analogue in cancer treatment.

Conclusions

AKR1C3 has a regulating role in several cellular proliferation and differentiation pathways. Overexpressed AKR1C3 can result in prolific PGs and androgens/oestrogens that influence gene transcription in several different cancers and diseases. The ability to inhibit overactive AKR1C3 could decrease cell proliferation while increasing differentiation and apoptosis.

Widely studied as a potential treatment option for cancer, curcumin has shown inhibitory activities on tumorous cell lines. However, due to its poor bioavailability and stability, it has not been terribly successful *in vivo*. This has led to the development and use of curcumin analogues with greater bioavailability and stability. Previous research has shown naturally occuring DMC and BDMC to be more potent than curcumin, suggesting they could be more effective in inhibiting AKR1C3. In an attempt to inhibit AKR1C3 activity in transformed *E. coli* cells, we used the polyphenol curcumin and its analogues DMC and BDMC.

Enzyme assays measuring the oxidation rate of the AKR1C3 co-activator NADPH found the inhibitor potency to be BDMC > DMC > curcumin, as seen in previous research. Further analysis of BDMC indicated a type of mixed inhibition. AKR1C3 activity was found to have a constant V_{max} in the presence and absence of BDMC, but a lower K_m in the presence of BDMC compared to the absence of BDMC. Additional experiments must be conducted to confirm this type of inhibition.

Interestingly, we observed AKR1C3 did not follow Michaelis-Menten kinetics at higher concentrations of substrate with or without an inhibitor. This indicates there may be a second binding site within the AKR1C3 enzyme that allows for self-inhibition, which has not yet been reported to our knowledge. This possibility could have great implications in drug development and targeting of AKR1C3 for cancer treatment. The crystal structure of AKR1C3 with PQ as its substrate should be explored above substrate saturation to determine if a hidden binding site is exposed. If so, this

potential binding site could be utilised in addition to AKR1C3 inhibitors, as the inhibitory effectiveness increased as the PQ substrate concentration increased.

In support of previous research, we found that BDMC is a more potent inhibitor of AKR1C3 activity in transformed *E. coli* cells. More data must be collected to confirm mixed inhibition, as curcumin and AKR1C3 has shown different inhibition activities depending on the molecule they are binding to. Further analysis of the structure of AKR1C3 must also be explored to determine if an additional binding site does not appear upon substrate saturation and lead to self-inhibition of the enzyme.

Acknowledgements

Thank you to Professor Frank Michelangeli for all of the support and advice provided throughout this process.

Abbreviations

AKR1C3: Aldo-keto reductase 1C3; BDMC: bisdemethoxycurcumin; DMC: demethoxycurcumin; PPARγ: peroxisome proliferator-activated receptor γ; PQ: 9,10-phenanthrenequionene.

References

1. Penning TM, Burczynski ME, Jez JM, Hung CF, Lin HK, Ma H, Moore M, Palackal N, Ratnam K. Human 3a-hydroxysteroid dehydrogenase isoforms (AKR1C1-AKR1C4) of the aldo-keto reductase superfamily: functional plasticity and tissue distribution reveals roles in the activation and formation of male and female sex hormones. Biochem J. 2000;351:67-77.
2. Yamada T, Watanabe K, Takusagawa F. Crystal structure of human prostaglandin F synthase (AKR1C3). Biochem. 2004;43:2188-98.
3. Suzuki-Yamamoto T, Nishizawa M, Fukui M, Okuda-Ashitaka E, Nakajima T, Ito S, Watanbe K. cDNA cloning, expression and characterization of human prostaglandin F synthase. FEBS Lett. 1999;462:335-40.
4. Yu CC, Huang SP, Lee YC, Huang CY, Liu CC, Hour TC, Huang CN, You BJ, Chang TY, et al. Molecular markers in sex hormone pathway genes associated with the efficacy of androgen-deprivation therapy for prostate cancer. PLos One. 2013;8:e54627.
5. Lin HK, Jez JM, Schlegel BP, Peehl DM, Pachter JA, Penning TM. Expression and characterization of recombinant type 2 3 alpha-hydroxysteroid dehydrogenase (HSD) from human prostate: demonstration of bifunctional 3 alpha/17 beta-HSD activity and cellular distribution. Mol Endocrinol. 1997;11:1971-84.
6. Penning TM. Aldo-Keto Reductase (AKR) 1C3 inhibitors: a patent review. Expert Opin Ther Pat. 2017;27:1329-40.
7. Penning TM. AKR1C3 (type 5 17β-hydroxysteroid dehydrogenase/prostaglandin F synthase): Roles in malignancy and endocrine disorders. Mol Cell Endorinol. 2019;489:82-91.
8. Matsunaga T, Hojo A, Yamane Y, Endo S, El-Kabbani O, Hara A. Pathopysiological roles of aldo-keto reductases (AKR1C1 and AKR1C3) in development of cisplatin resistance in human colon cancers. Chem-Biol Interact. 2013;202:234-42.
9. Desmond JC, Mountford JC, Drayson MT, Walker EA, Hewison M, Ride JP, Loung QT, Hayden RE, Vanin EF, Bunce CM. The aldo-keto reductase AKR1C3 is a novel suppressor of cell differentiation that provides a plausible target for the non-cyclooxygenase-dependent antineoplastic actions of nonsteroidal anti-inflammatory drugs. Cancer Res. 2003;63:505-12.
10. Shiraki T, Kamiya N, Shiki S, Kodama TS, Kakizuka A, Jingami H. α,β-Unsaturated Ketone Is a Core Moiety of Natural Ligands for Covalent Binding to Peroxisome Proliferator-activated Receptor γ. J Biol Chem. 2005;280:14145-53.
11. Sandur SK, Ichikawa H, Pandey MK, Kunnumakkara AB, Sung B, Sethi G, Aggarwal BB. Role of Prooxidants and Antioxidants in the Anti-Inflammatory and Apoptotic Effects of Curcumin (Diferuloylmethane). Free Radic Biol Med. 2007;43:568-80.
12. Tomeh MA, Hadianamrei R, Zhao X. A Review of Curcumin and Its Derivatives as Anticancer Agents. Int J Mol Sci. 2019;20:1033.
13. Sandur SK, Pandey MK, Sung B, Ahn KS, Murakami A, Sethi G, Limtrakul P, Badmaev V, Aggarwal BB. Curcumin, demethoxycurcumin, bisdemethoxycurcumin, tetrahydrocurcumin and tumerones differentially regulate anti-inflammatory and anti-proliferative responses through a ROS-independent mechanism. Carcinogenesis. 2007;28:1765-73.
14. Cheng AL, Hsu CH, Lin JK, Hsu MM, Ho YF, Shen TS, Ko JY, Lin JT, Lin BR, et al. Phase I clinical trial of curcumin, a chemopreventive agent, in patients with high-risk or pre-malignant lesions. Anticancer Res. 2001;21:2895-900.
15. Hoehle SI, Pfeiffer E, Solyom AM, Metzier M. Metabolism of curcuminoids in tissue slices and subcellular fractions from rat liver. J Agric Food Chem. 2006;54:756-64.

16. Price LC, Buesher RW. Decomposition of turmeric curcuminoids as affected by light, solvent, and oxygen. J Biol Chem. 1996;20:125-133.
17. Yodkeeree S, Chaiwangyen W, Garbisa S, Limtrakul P. Curcumin, demethoxycurcumin and bisdemthoxycurcumin differentially inhibit cancer cell invasion through the down-regulation of MMPs and uPA. J Nutr Biochem. 2009;20:87-95.
18. Ide H, Lu Y, Noguchi T, Muto S, Okada H, Kawato S, Horle S. Modulation of AKR1C2 by curcumin decreases testosterone production in prostate cancer. Cancer Science. 2018;109:1230-38.
19. Byrns MC, Jin Y, Penning TM. Inhibitors of type 5 17β-hydroxysteroid dehydrogenase (AKR1C3): Overview and structural insights. J Steroid Biochem Mol Biol. 2011;125:95-104.
20. Lovering AL, Ride JP, Bunce CM, Desmond JC, Cummings SM, White SA. Crystal Structures of Prostaglandin D_2 11-Ketoreductase (AKR1c3) in Complex with the Nonsteroidal Anti-Inflammatory Drugs Flufenamic Acid and Indomethacin. Cancer Res. 2004;64:1802-10.
21. Appiah-Opong R, Commandeur JN, van Vugt-Lussenburg B, Vermeulen NP. Inhibition of human recombinant cytochrome P450s by curcumin and curcumin decomposition products. Toxicology. 2007;235:83-91.
22. Reddy S, Aggarwal BB. Curcumin is a non-competitive and selective inhibitor of phosphorylase kinase. FEBS Lett. 1994;341:19-22.
23. Zang T, Verma K, Chen M, Jin Y, Trippier PC, Penning TM. Screening baccharin analogs as selective inhibitors against type 5 17β-hydroxysteroid dehydrogenase (AKR1C3). Chem Biol Interact. 2015;234:339-48.
24. Yoda T, Kikuchi K, Miki Y, Onodera Y, Hata S, Takagi K, Nakamura Y, Hirakawa H, Ishida T, et al. 11β-Prostaglandin F2a, a bioactive metabolite catalyzed by AKR1C3, stimulates prostaglandin F receptor and induces slug expression in breast cancer. Mol Cell Endocrinol. 2015;413:236-47.
25. Komoto J, Yamada T, Watanabe K, Takusagawa F. Crystal Structure of Human Prostaglandin F Synthase (AKR1C3). Biochemistry. 2004;43:2188-98.
26. Jabbour H.N., Sales KJ. Prostaglandin receptor signaling and function in human endometrial pathology. Trends Endocrinol Metab. 2004;15:3980404.
27. Coutinho I, Day TK, Tilley WD, Selth LA. Androgen receptor signaling in castration-resistant prostate cancer: a lesson in persistence. Endocr Relat Cancer. 2016;23:T179-97.
28. Desmond JC, Mountford JC, Drayson MT, Walker EA, Hewison M, Ride JP, Loung QT, Hayden RE, Vanin EF, Bunce CM. The aldo-keto reductase AKR1C3 is a novel suppressor of cell differentiation that provides a plausible target for the non-cyclooxygenase-dependent antineoplastic actions of nonsteroidal anti-inflammatory drugs. Cancer Res. 2003;63:505-12.
29. Reginato MJ, Krakow SL, Bailey ST, Lazar MA. Prostaglandins promote and block adipogenesis through opposing effects on peroxisome proliferator-activated receptor gamma. J Biol Chem. 1998;273:1855-8.
30. Kliewer SA, Lenhard JM, Willson TM, Patel I, Morris DC, Lehmann JM. A prostaglandin J_2 metabolite binds peroxisome proliferator-activated receptor γ and promotes adipocyte differentiation. Cell. 1995;83:813-19.
31. Cornago P, Claramunt RM, Bouissane L, Alkorta I, Elguero J. A study of the tautomerism of beta-dicarbonyl compounds with special emphasis on curcuminoids. Tetrahedron. 2008;64:8089-94.
32. Bertolasi V, Ferretti V, Gilli P, Yao X, Li CJ. Substituent effects on keto-enol tautomerization of [small-beta]-diketones from X-ray structural data and DFT calculations. New J Chem. 2008;32:694-704.
33. Jovanovic SV, Steenken S, Boone CW, Simic MG. H-atom transfer is preferred antioxidant mechanism of curcumin. J Am Chem Soc. 1999;121:9677-9681.
34. Lee WH, Loo CY, Bebawy M, Luk F, Mason RS, Rohanizadeh R. Curcumin and its derivatives: Their application in neuropharmacology and neuroscience in the 21st century. Curr Neuropharmacol. 2013;11:338-78.
35. Priyadarsini, KI. Photophysics, photochemistry and photobiology of curcumin: Studies from organic solutions, bio-memetics and live cells. J Photochem Photobiol C. 2009;10:81-95.